

# View-Invariant Gait Representation Using Joint Bayesian Regularized Non-negative Matrix Factorization

Maryam Babaei, Gerhard Rigoll

Institute for Human-Machine Communication, TU Munich, Germany

maryam.babaei@tum.de, rigoll@tum.de

## Abstract

*Gait as a biometric feature has been investigated for human identification and biometric application. However, gait is highly dependent on the view angle. Therefore, the proposed gait features do not perform well when a person is changing his/her orientation towards camera. To tackle this problem, we propose a new method to learn low-dimensional view-invariant gait feature for person identification/verification. We model a gait observed by several different points of view as a Gaussian distribution and then utilize a function of Joint Bayesian as a regularizer coupled with the main objective function of non-negative matrix factorization to map gait features into a low-dimensional space. This process leads to an informative gait feature that can be used in a verification task. The performed experiments on a large gait dataset confirms the strength of the proposed method.*

## 1. Introduction

Recently, employing gait (the way of natural walking) for individual identification has been drawing significant attention in the field of video surveillance and biometric applications [24, 11, 3]. Compared to the traditional biometrics based on face, fingerprint or iris, gait has been considered as a more promising and unique biometric for person identification, due to its capability in identifying a person even in low resolution images captured from a large distance [14]. Many gait representation methods have been proposed which are invariant to body shape that are able to extract the useful information of a walking sequence [4, 5, 16, 17, 19]. However, these gait features are influenced by viewing angle of the used cameras. Apparently, the gait signature of different persons should be still distinguishable and robust when the viewing angle is changed. Therefore, having a view-invariant (or cross-view) gait feature is highly desirable in video surveillance applications, where the orientation of movement is chang-

ing toward the installed static (dynamic) cameras. Basically, the output of most well known hand-crafted gait features is a silhouette image representing a full gait cycle. The high dimensionality of these features leads to computationally expensive gait recognition systems. Moreover, since a big portion of a silhouette image are zero pixels, the required memory in real time applications is very high.

In this paper, we aim to have a gait representation which addresses the two aforementioned issues. We propose a feature learning technique based on Non-negative Matrix Factorization (NMF), where the learned gait features of an individual observed from different views would have high similarity. Inspired by Joint Bayesian (JB) for face verification [9], we utilize the Joint Bayesian formulation in order to model the view variance. Specifically, we assume that the joint probability of two gait feature of different views is a Gaussian distribution. Based on this assumption, we compute the log-likelihood of joint probability by MAP (Maximum a Posterior) as similarity term. We utilize this term [9] as a regularizer coupled with Non-negative Matrix Factorization (NMF) [8] to come up with a novel NMF technique that maps a view-variant high-dimensional gait feature into a new low-dimensional view-invariant gait feature, meanwhile the performance of gait verification is significantly improved.

The rest of the paper is structured as follows. In Section 2, we provide a review of the state-of-the-art methods in the area of gait recognition and verification. In Section 3, we propose our algorithm by first explaining a similarity score based on Joint Bayesian and then its usage as a regularizer in NMF. Section 4 provides the experimental results of the proposed algorithm for gait verification. Finally, we draw our conclusion in Section 5.

## 2. Related work

In gait recognition, there are different methods for gait representation. Traditional gait features such as Gait Energy Image (GEI) [20], Gait Entropy Image (GENI) [5], Enhanced Gait Energy Image (EGEI) [10], Gait Flow Image

(GFI) [16], Masked GEI (MGEI) [6] represent a gait cycle (i.e., several silhouette images) by a single image. For instance, as a simple but effective feature, GEI is the average over a complete gait cycle silhouettes. The EGEI method analyzes the dynamic region information to enhance GEI feature. GENI represents the randomness of pixel values in the silhouettes image sequence. GFI is generated by using an optical flow field. MGEI feature is obtained by masking GEI with gait entropy image. However, these are very high-dimensional features, which could be undesirable for real time applications and are significantly depended on the view point.

For modeling view variance, different approaches have been proposed including view transformation model (VTM) [23, 22], view invariant feature based classification [25, 15], and multiple view gallery based methods [7, 13]. Besides, Deep Learning methods have also been recently applied to gait representation. In [26], Wolf *et al.* present a 3D Convolutional Neural Network (CNN) to attain a human gait descriptor invariant to view angles. Similarly, a CNN called GEInet was designed in [25], which gets GEI feature as input and outputs a set of similarity score to training subject data. This network shows also promising results in terms of view variance. As a different approach for verification task, Moghaddam *et al.* in [21] formulate the verification problem as classifying the appearance difference between two images in face recognition. They propose a probabilistic similarity score based on Bayesian analysis of images' differences.

Amongst the most well known matrix factorization methods like Principal Component Analysis (PCA) and Singular Value Decomposition (SVD), NMF has been also employed widely in computer vision. Depending on the application, many variants of NMF have been proposed. For instance, Graph regularized NMF (GNMF) [8] tries to maintain the locality of the data points by defining the Laplacian of neighborhood graph as a regularizer the objective function. In [2, 1], a semi supervised NMF, named Discriminative NMF, was proposed which utilizes the label of a fraction of data as a discriminative constraint. Here, the data points with the same label are in one axis or close to each other, despite of constrained NMF (CNMF) [18], where all these points are merged to a single point in the new low-dimension space.

### 3. Approach

In this section, we first review the Joint Bayesian formulation in order to model view variance in gait features. Then, a similarity function based on Joint Bayesian is proposed as a regularizer in Non-negative matrix factorization to generate view-invariant gait features.

#### 3.1. Joint Bayesian

The Joint Bayesian approach has been proved as a successful technique in dealing with view-invariant face verification [9]. According to the same idea, we represent a gait cycle feature by the sum of two independent Gaussian variables:

$$x = \mu + \varepsilon \quad (1)$$

where  $x$  is the zero-mean observed gait feature,  $\mu$  represents its identity, and  $\varepsilon$  is the gait variation of the same identity observed by a different view. We assume that  $\mu$  and  $\varepsilon$  both are coming from Gaussian distributions,  $N(0, S_\mu)$  and  $N(0, S_\varepsilon)$ , respectively. Here,  $S_\mu$  and  $S_\varepsilon$  are covariance matrices. Therefore, the joint distribution of  $x_1, x_2$  has also a Gaussian distribution with zero mean. Under intra-personal hypothesis  $H_I$ , when two gait features belong to the same class, the identities of  $x_1$  and  $x_2$  are the same and their intra-person variations are independent. Then, the covariance matrix of the distribution  $P(x_1, x_2 | H_I)$  can be derived as:

$$\Sigma_I = \begin{bmatrix} S_\mu + S_\varepsilon & S_\mu \\ S_\mu & S_\mu + S_\varepsilon \end{bmatrix} \quad (2)$$

Under extra-personal hypothesis  $H_E$ , when two gait features do not belong to the same class, both the identities and intra-person variations are independent. Then, the covariance matrix of the distribution  $P(x_1, x_2 | H_E)$  is:

$$\Sigma_E = \begin{bmatrix} S_\mu + S_\varepsilon & 0 \\ 0 & S_\mu + S_\varepsilon \end{bmatrix}. \quad (3)$$

Based on the two conditional joint probabilities above, the log-likelihood ratio  $r(x_1, x_2)$  can be obtained as [9]:

$$\begin{aligned} r(x_1, x_2) &= \log \frac{P(x_1, x_2 | H_I)}{P(x_1, x_2 | H_E)} \\ &= x_1^T A x_1 + x_2^T A x_2 - 2x_1^T G x_2 \end{aligned} \quad (4)$$

where

$$A = (S_\mu + S_\varepsilon)^{-1} - (F + G) \quad (5)$$

and

$$\begin{bmatrix} F + G & G \\ G & F + G \end{bmatrix} = \begin{bmatrix} S_\mu + S_\varepsilon & 0 \\ 0 & S_\mu + S_\varepsilon \end{bmatrix}^{-1}. \quad (6)$$

By using an efficient Inverse, we have

$$F = S_\varepsilon^{-1}, \quad (7)$$

$$G = -(2S_\mu + S_\varepsilon)^{-1} S_\mu S_\varepsilon^{-1}, \quad (8)$$

$$A = (S_\mu + S_\varepsilon)^{-1} - S_\varepsilon^{-1} + (2S_\mu + S_\varepsilon)^{-1} S_\mu S_\varepsilon^{-1}. \quad (9)$$

This ratio  $r$  is considered as the amount of similarity between two gait features.

### 3.2. Joint Bayesian Regularized NMF

Non-negative matrix factorization (NMF) has drawn a significant attention in recent years for representation of high-dimensional data. NMF aims to factorize an input matrix to two (three) non-negative matrices whose product provides a good approximation to the input matrix.

$$X \approx UV \quad (10)$$

Here  $X$  is a data matrix,  $X \in \mathbb{R}^{M \times N}$ ,  $U \in \mathbb{R}^{M \times K}$  and  $V \in \mathbb{R}^{K \times N}$ .  $N$  is the number of data samples, and  $M$  is the size of feature vector in original space. The dimension of the data in the new space would be  $K$ . A cost function, which can be used for quantifying the quality of the approximation, is the square of the Frobenius norm of the difference of two matrices.

$$\begin{aligned} O_F &= \|X - UV\|^2 \\ \text{s.t. } U &= [u_{ik}] \geq 0, \quad V = [v_{kj}] \geq 0 \end{aligned} \quad (11)$$

Denoting  $Tr(\cdot)$  as the trace of a matrix, this objective function can be rewritten as:

$$\begin{aligned} O_F &= \|X - UV\|^2 = \sum_{i,j} (x_{ij} - \sum_{k=1}^K u_{ik}v_{kj})^2 \\ &= Tr(XX^T) - 2Tr(XV^T U^T) + Tr(UVV^T U^T). \end{aligned} \quad (12)$$

NMF can learn a parts-based representation using the non-negative constraints, but it does not take the intrinsic relation and dissimilarity of low-dimensional representations of data points into consideration.

In the following part, we introduce our approach based on the combination of NMF and JB which avoids this limitation. We modify the objective function so that the sum of similarity score (i.e., ratio  $r$  defined by 4) of all pairs of gait features from the same class is maximum. In other words, a low-dimensional gait feature is desirable, where the features of the same class but different views have a high similarity score. Hereby, the objective function would be:

$$O = \|X - UV\|^2 - \frac{\alpha}{2} \sum_{i,j=1}^N r(v_i, v_j) w_{ij}, \quad (13)$$

where  $X$  contains high-dimensional view-variant gait features, and  $V$  is the low-dimensional view-invariant gait features ( $V = \{v_1, v_2, \dots, v_N\}$ ).  $W$  is a 0-1 weight matrix.  $w_{ij} = 1$  if and only if the gait features  $i$  and  $j$  belong to the same class. For the derivation of update rules, we expand

the objective function in equation 13 to

$$\begin{aligned} O &= \|X - UV\|^2 - \frac{\alpha}{2} \sum_{i,j=1}^N (v_i^T \tilde{A} v_i + v_j^T \tilde{A} v_j - 2v_i^T \tilde{G} v_j) w_{ij} \\ &= \|X - UV\|^2 - \alpha \sum_{i=1}^N (v_i^T \tilde{A} v_i) w_{ii} + \alpha \sum_{i,j=1}^N (v_i^T \tilde{G} v_j) w_{ij} \\ &= \|X - UV\|^2 - \alpha Tr(DV_0^T \tilde{A} V_0) + \alpha Tr(WV_0^T \tilde{G} V_0). \end{aligned} \quad (14)$$

where  $V_0$  is zero-mean matrix  $V$ , and  $D$  is a diagonal matrix whose entries are column sums of  $W$ .  $\tilde{A}$  and  $\tilde{G}$  are Joint Bayesian model matrices in the new space. By employing equation 12, our objective function would be:

$$\begin{aligned} O &= Tr(XX^T) - 2Tr(XV^T U^T) + Tr(UVV^T U^T) \\ &\quad - \alpha Tr(DV_0^T \tilde{A} V_0) + \alpha Tr(WV_0^T \tilde{G} V_0), \end{aligned} \quad (15)$$

Let  $\phi_{ik}$  and  $\psi_{kj}$  be the Lagrange multiplier for constraints  $u_{ik} \geq 0$  and  $v_{kj} \geq 0$ , respectively, and also  $\Phi = [\phi_{ik}]$ ,  $\Psi = [\psi_{kj}]$ , then Lagrange  $\mathcal{L}$  is

$$\begin{aligned} \mathcal{L} &= Tr(XX^T) - 2Tr(XV^T U^T) + Tr(UVV^T U^T) \\ &\quad + Tr(\Phi U) + Tr(\Psi V) - \alpha Tr(DV_0^T \tilde{A} V_0) \\ &\quad + \alpha Tr(WV_0^T \tilde{G} V_0). \end{aligned} \quad (16)$$

According to [9], under linear transformation, then we get the following relationships;

$$\tilde{A} = U^T A U^{-T}, \quad \tilde{G} = -U^T G U \quad (17)$$

where  $A$  and  $G$  are Joint Bayesian model in original space. Considering equation 17, the partial derivatives of  $\mathcal{L}$  with respect to  $U$  and  $V$  are:

$$\begin{aligned} \frac{\partial \mathcal{L}}{\partial U} &= -2XV^T + 2UVV^T + \Phi \\ &\quad - \alpha(-U^{-T} V_0 D X_0^T A U^{-T}) + \alpha(-G^T X_0 W^T V_0^T) \end{aligned} \quad (18)$$

$$\begin{aligned} \frac{\partial \mathcal{L}}{\partial V} &= -2U^T X + 2U^T U V + \Psi \\ &\quad - \alpha(U^{-1} A^T X_0 D^T) + \alpha(-U^T G^T X_0 W^T) \end{aligned} \quad (19)$$

Using the KKT conditions  $\phi_{ik} u_{ik} = 0$  and  $\psi_{kj} v_{kj} = 0$ , the new updating rules of  $U$  and  $V$  are obtained as:

$$u_{ik} \leftarrow u_{ik} \frac{(2XV^T + \alpha G^T X_0 W^T V_0^T)_{ik}}{(2UVV^T + \alpha U^{-T} V_0 D X_0^T A U^{-T})_{ik}} \quad (20)$$

$$v_{kj} \leftarrow v_{kj} \frac{(2U^T X + \alpha U^{-1} A^T X_0 D^T + \alpha U^T G^T X_0 W^T)_{kj}}{(2U^T U V)_{kj}} \quad (21)$$

Then the matrix  $V$  contains low-dimensional view-invariant gait features.

## 4. Experiment

In order to evaluate our approach, we conduct several experiments for verification tasks on a gait dataset. In Section 3.2, we have introduced our feature learning method, considering a Joint Bayesian based regularizer in the NMF objective function. To measure the quality of learned feature, we report verification rates obtained from original and new gait features.

### 4.1. Dataset

The OU-ISIR Large Population dataset (OULP) [12], which includes high-quality images with view variations, is utilized in our research. This dataset consists of images showing persons walking on the ground and is basically distributed in a form of silhouette sequences registered and size-normalized to 88\*128 pixels. Each subject is further divided into 4 subsets based on the observation view angles, namely 55°, 65°, 75° and 85°. There are two samples for each angle, that one of them is used as gallery and another one for probe. Figure 1 shows four gait cycle samples of a subject from this dataset observed from different view angles.

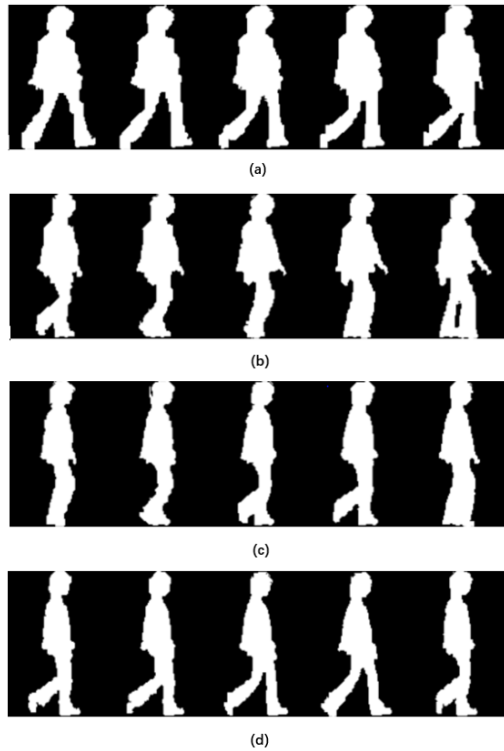


Figure 1: Silhouette sequences of a gait cycle of a person observed by different angles, namely (a) 55°, (b) 65°, (c) 75°, (d) 85°

### 4.2. Setting

First, the silhouette images are re-sized into 44\*64 pixels in favor of decreasing computational complexity. Then we extract five different well known gait features, namely GEI, GEnI, MGEI, EGEI, and GFI from each gait cycle. Figure 2 depicts the GEI features of a particular subject viewed from different angles. Due to the high dimensionality of

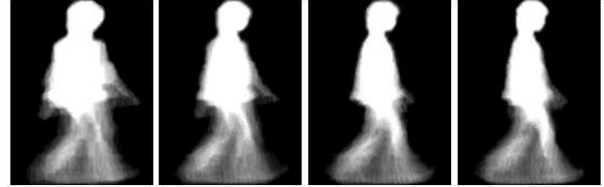


Figure 2: GEI gait feature of a subject viewed by four different angles (left to right: 55°, 65°, 75°, 85°)

these features, we apply PCA to reduce the dimensionality to  $K$ . In our experiments, we select randomly 1600 samples categorized as 200 subjects from OULP dataset due to high computational time. Each subject has 2 gait cycle samples (one for gallery and one for probe) per view angle. To compare the result of NMF with PCA,  $K$  is also set to 200 (number of subjects), since the feature dimensionality of NMF equals to the number of subjects. The value of regularization multiplier ( $\alpha$ ) in our objective function is set to 100 (this value has been obtained by cross-validation procedure).

The verification experiments are implemented among different cross-view combinations. For verification, we consider two similarity metrics for gait features: 1) log-likelihood ratio ( $Dist_{LLR}$ ) and 2) Euclidean distance ( $Dist_{Euc}$ ). The formula of computing each similarity metric is given by

$$Dist_{LLR}(x_1, x_2) = -\log \frac{P(x_1, x_2 | H_I)}{P(x_1, x_2 | H_E)} \quad (22)$$

$$Dist_{Euc}(x_1, x_2) = \left\| \frac{x_1}{\|x_1\|} - \frac{x_2}{\|x_2\|} \right\| \quad (23)$$

In the experiment, we consider different non/cross-view combinations of gallery and probe pairs. For each combination, first the similarity score of each probe sample with each gallery subject is calculated and then the corresponding Equal Error Rate (EER) for this combination is computed. The verification results based on  $Dist_{LLR}$  and  $Dist_{Euc}$  are presented in Tables 1 and 2, respectively. Additionally, the Receiver Operative Characteristics (ROC) curve of False Acceptance Rates (FAR) and False Rejection Rates (FRR) for both similarity metrics under different cross-view settings are presented in Figure 3.

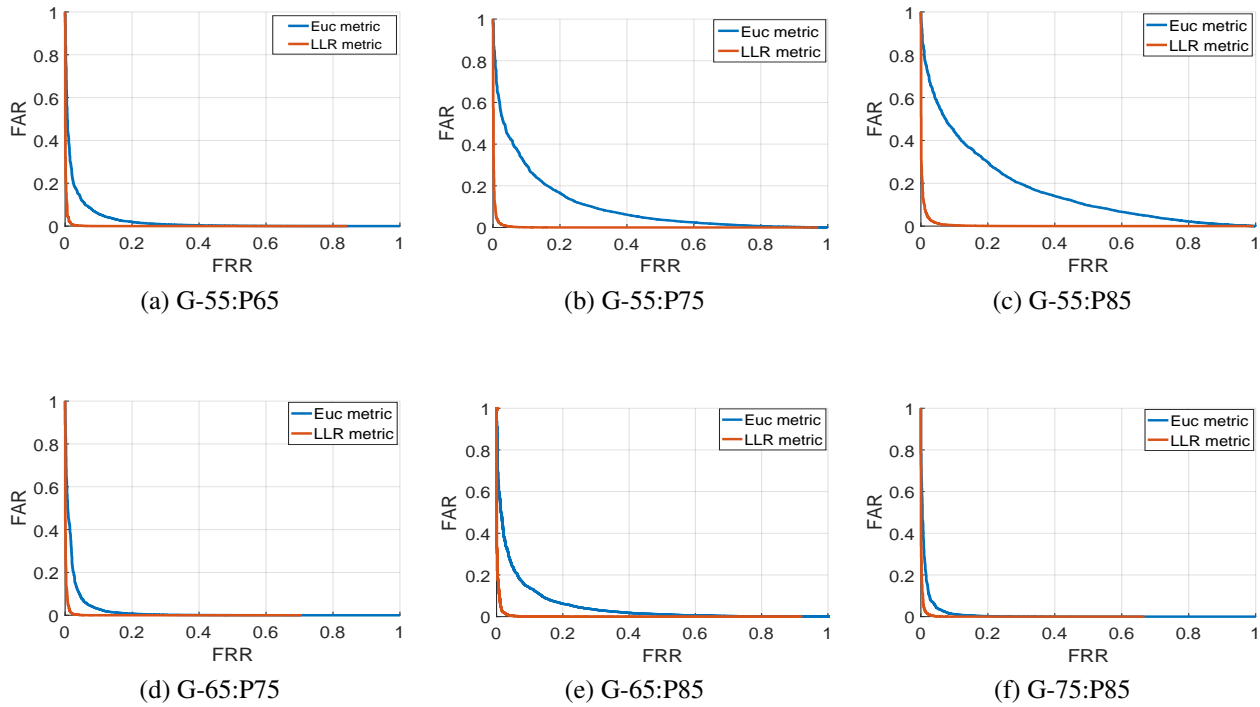


Figure 3: ROC curves under different cross-view settings of GEI

### 4.3. Results and discussion

The obtained results demonstrate that gait cycles are more reliably verified when they are represented by our algorithm. By comparing the results of using two similarity metrics (Tables 1 and 2), it can be found that using the log-likelihood ratio as the similarity score gives us this ability to do the verification task more accurately even in the presence of a large view variation. More specifically, referring to Tables 1 and 2, it can be inferred that: 1) The gait cycles represented by our proposed method (NMF+JB) can be verified with a higher performance, compared to PCA. For example, the EER corresponding to pair (55°, 65°), using gallery set with view angle 55° and probe set with view angle 65°, decreased from 16.43% to 7.86%, for GEI as input feature representation. This statement is true for every non/cross view combination; 2) According to Table 2, the EER remains relatively low at the same level for different non/cross view combinations; 3) The obtained results for different gait representations show that the verification performance of our proposed method is relatively independent from the type of input gait feature. ROC curves for different cross-view combinations in Figure 3 show that the verification based on the log-likelihood ratio measure outperforms the verification using the Euclidean distance measure. Moreover, in cross-view with a larger difference in

camera viewing angle, for example gallery 55° and probe 85°, this distinction is significant. Last but not the least, it can be seen that the performance of verification based on log-likelihood ratio remains at the same level in this set of combinations, while ROC curves for second approach (verification based on euclidean distance) differ on the view distance.

### 5. Conclusion

We proposed a new method to generate view-invariant gait features based on NMF. We employed a regularizer based on Joint Bayesian and attached to the main objective function of NMF. We conducted several gait verification experiments on the OULP gait dataset represented by different gait features. We considered two types of similarity metrics, namely log-likelihood ratio and Euclidean distance. The results confirmed that our method has achieved better performance, apart from the type of gait features used as input. Additionally, we found out that verification based on the log-likelihood ratio performs more stably than verification based on the Euclidean distance. For future work, we intend to examine our approach on gait identification as well as gait verification against further variances such as clothing and a larger view variation.

Gallery View	Gait Cycle Representation	PCA				NMF+JB			
		55	65	75	85	55	65	75	85
55	GEI	6.89	16.43	31.63	37.95	<b>3.55</b>	7.86	18.07	24.31
	GEnI	6.81	17.95	32.74	38.68	<b>3.24</b>	10.67	23.11	29.34
	MGEI	5.30	16.73	29.31	32.93	<b>4.15</b>	13.74	24.3	26.36
	EGEI	6.99	18.11	32.57	38.40	<b>3.72</b>	11.04	23.28	28.14
	GFI	6.78	14.99	28.39	34.98	<b>5.31</b>	9.87	20.01	26.96
65	GEI	17.21	5.80	11.63	21.07	8.05	<b>3.95</b>	6.05	11.9
	GEnI	18.83	6.10	12.59	22.81	11.05	<b>3.81</b>	6.81	14.99
	MGEI	14.63	4.60	9.88	18.33	13.41	<b>4.60</b>	9.45	15.56
	EGEI	19.09	6.16	12.85	22.96	11.41	<b>3.65</b>	7.26	14.91
	GFI	15.35	5.95	10.35	17.87	9.83	<b>5.70</b>	7.87	13.01
75	GEI	31.47	11.90	5.44	7.35	18.87	6.20	<b>3.75</b>	4.46
	GEnI	33.37	12.82	5.17	7.71	24.44	7.36	<b>3.35</b>	4.15
	MGEI	29.10	9.71	4.10	5.68	24.39	8.78	<b>3.95</b>	5.82
	EGEI	33.11	13.13	5.44	8.02	23.72	4.42	<b>3.31</b>	4.45
	GFI	28.12	10.36	5.42	7.29	20.14	7.84	<b>4.96</b>	6.18
85	GEI	37.55	21.33	7.36	5.38	25.21	12.26	4.40	<b>3.15</b>
	GEnI	38.90	23.38	8.27	5.61	29.90	15.95	4.45	<b>2.80</b>
	MGEI	32.93	18.06	5.96	4.71	26.96	15.22	5.36	<b>3.61</b>
	EGEI	38.28	23.20	8.52	5.74	28.67	15.56	4.35	<b>2.93</b>
	GFI	34.78	18.40	7.24	5.68	27.53	13.17	5.39	<b>4.35</b>

Table 1: Comparison of EERs (%) in gait verification based on  $Dist_{Euc}$  metric, after applying PCA and NMF+JB transformations on different gait features under cross-view and non cross-view settings

Gallery View	Gait Cycle Representation	PCA				NMF+JB			
		55	65	75	85	55	65	75	85
55	GEI	2.71	2.79	2.88	4.48	<b>1.31</b>	1.62	2.05	2.85
	GEnI	3.23	3.07	4.28	6.53	<b>1.96</b>	1.97	2.70	3.73
	MGEI	3.75	3.53	5.03	6.70	2.20	<b>2.16</b>	2.94	4.04
	EGEI	3.38	3.16	4.29	6.48	1.94	<b>1.80</b>	2.40	3.46
	GFI	3.09	2.82	3.46	5.16	2.20	<b>2.10</b>	2.49	3.53
65	GEI	2.76	2.29	2.11	3.23	1.65	<b>1.37</b>	1.60	2.10
	GEnI	3.44	2.55	2.99	4.04	2.20	<b>1.75</b>	2.01	2.57
	MGEI	4.09	3.12	3.39	4.89	2.50	<b>1.90</b>	2.40	3.08
	EGEI	3.43	2.50	2.84	4.08	2.11	<b>1.46</b>	1.95	2.35
	GFI	3.06	2.41	2.69	3.56	1.91	<b>1.66</b>	1.91	2.36
75	GEI	2.96	2.26	2.10	2.41	2.11	<b>1.40</b>	1.55	1.69
	GEnI	3.92	2.75	2.52	3.35	2.26	1.66	<b>1.60</b>	2.01
	MGEI	5.41	3.08	3.02	3.89	2.85	<b>1.65</b>	1.95	2.61
	EGEI	3.87	2.64	2.52	3.19	2.30	<b>1.65</b>	1.70	2.10
	GFI	3.40	2.38	2.33	2.65	2.35	1.75	<b>1.65</b>	2.07
85	GEI	4.03	2.57	2.41	2.44	2.75	1.60	<b>1.46</b>	1.65
	GEnI	5.31	3.50	2.71	2.72	2.80	1.89	2.05	<b>1.80</b>
	MGEI	6.51	3.73	3.38	3.62	3.49	2.36	2.26	<b>2.25</b>
	EGEI	5.34	3.49	2.67	2.77	3.05	2.01	<b>1.75</b>	1.85
	GFI	4.08	2.78	2.58	2.53	3.36	2.12	2.17	<b>1.90</b>

Table 2: Comparison of EERs (%) in gait verification based on  $Dist_{LLR}$  metric, after applying PCA and NMF+JB transformations on different gait features under cross-view and non cross-view settings

## References

- [1] M. Babae, R. Bahmanyar, G. Rigoll, and M. Datcu. Farness preserving non-negative matrix factorization. In *Image Processing (ICIP), 2014 IEEE International Conference on*, pages 3023–3027. IEEE, 2014.
- [2] M. Babae, S. Tsoukalas, M. Babae, G. Rigoll, and M. Datcu. Discriminative nonnegative matrix factorization for dimensionality reduction. *Neurocomputing*, 173:212–223, 2016.
- [3] A. Babaeian, M. Babae, A. Bayestehtashk, and M. Bandarabadi. Nonlinear subspace clustering using curvature constrained distances. *Pattern Recognition Letters*, 68:118–125, 2015.
- [4] R. V. Babu and K. Ramakrishnan. Recognition of human actions using motion history information extracted from the compressed video. *Image and Vision computing*, 22(8):597–607, 2004.
- [5] K. Bashir, T. Xiang, and S. Gong. Gait recognition using gait entropy image. 2009.
- [6] K. Bashir, T. Xiang, and S. Gong. Gait recognition without subject cooperation. *Pattern Recognition Letters*, 31(13):2052–2060, 2010.
- [7] R. Bodor, A. Drenner, D. Fehr, O. Masoud, and N. Papanikolopoulos. View-independent human motion classification using image-based reconstruction. *Image and Vision Computing*, 27(8):1194–1206, 2009.
- [8] D. Cai, X. He, J. Han, and T. S. Huang. Graph regularized nonnegative matrix factorization for data representation. *IEEE Transactions on Pattern Analysis and Machine Intelligence*, 33(8):1548–1560, 2011.
- [9] D. Chen, X. Cao, L. Wang, F. Wen, and J. Sun. Bayesian face revisited: A joint formulation. *Computer Vision–ECCV 2012*, pages 566–579, 2012.
- [10] L. Chunli and W. Kejun. A behavior classification based on enhanced gait energy image. In *Networking and Digital Society (ICNDS), 2010 2nd International Conference on*, volume 2, pages 589–592. IEEE, 2010.
- [11] M. O. Derawi, C. Nickel, P. Bours, and C. Busch. Unobtrusive user-authentication on mobile phones using biometric gait recognition. In *Intelligent Information Hiding and Multimedia Signal Processing (IIH-MSP), 2010 Sixth International Conference on*, pages 306–311. IEEE, 2010.
- [12] H. Iwama, M. Okumura, Y. Makihara, and Y. Yagi. The ou-isir gait database comprising the large population dataset and performance evaluation of gait recognition. *IEEE Transactions on Information Forensics and Security*, 7(5):1511–1521, 2012.
- [13] Y. Iwashita, R. Baba, K. Ogawara, and R. Kurazume. Person identification from spatio-temporal 3d gait. In *Emerging Security Technologies (EST), 2010 International Conference on*, pages 30–35. IEEE, 2010.
- [14] G. Johansson. Visual perception of biological motion and a model for its analysis. *Perception & psychophysics*, 14(2):201–211, 1973.
- [15] A. Kale, A. R. Chowdhury, and R. Chellappa. Towards a view invariant gait recognition algorithm. In *Advanced Video and Signal Based Surveillance, 2003. Proceedings. IEEE Conference on*, pages 143–150. IEEE, 2003.
- [16] T. H. Lam, K. H. Cheung, and J. N. Liu. Gait flow image: A silhouette-based gait representation for human identification. *Pattern recognition*, 44(4):973–987, 2011.
- [17] T. H. Lam and R. S. Lee. A new representation for human gait recognition: Motion silhouettes image (msi). In *International Conference on Biometrics*, pages 612–618. Springer, 2006.
- [18] H. Liu, Z. Wu, X. Li, D. Cai, and T. S. Huang. Constrained nonnegative matrix factorization for image representation. *IEEE Transactions on Pattern Analysis and Machine Intelligence*, 34(7):1299–1311, 2012.
- [19] J. Liu and N. Zheng. Gait history image: a novel temporal template for gait recognition. In *Multimedia and Expo, 2007 IEEE International Conference on*, pages 663–666. IEEE, 2007.
- [20] J. Man and B. Bhanu. Individual recognition using gait energy image. *IEEE transactions on pattern analysis and machine intelligence*, 28(2):316–322, 2006.
- [21] B. Moghaddam, T. Jebara, and A. Pentland. Bayesian face recognition. *Pattern Recognition*, 33(11):1771–1782, 2000.
- [22] D. Muramatsu, Y. Makihara, and Y. Yagi. Cross-view gait recognition by fusion of multiple transformation consistency measures. *IET Biometrics*, 4(2):62–73, 2015.
- [23] D. Muramatsu, Y. Makihara, and Y. Yagi. View transformation model incorporating quality measures for cross-view gait recognition. *IEEE transactions on cybernetics*, 46(7):1602–1615, 2016.
- [24] T. T. Ngo, Y. Makihara, H. Nagahara, Y. Mukaigawa, and Y. Yagi. The largest inertial sensor-based gait database and performance evaluation of gait-based personal authentication. *Pattern Recognition*, 47(1):228–237, 2014.
- [25] K. Shiraga, Y. Makihara, D. Muramatsu, T. Echigo, and Y. Yagi. Geinet: View-invariant gait recognition using a convolutional neural network. In *Biometrics (ICB), 2016 International Conference on*, pages 1–8. IEEE, 2016.
- [26] T. Wolf, M. Babae, and G. Rigoll. Multi-view gait recognition using 3d convolutional neural networks. In *Image Processing (ICIP), 2016 IEEE International Conference on*, pages 4165–4169. IEEE, 2016.